Competing Channels in Single-Electron Tunneling through a Quantum Dot

J. Weis, R. J. Haug, K. v. Klitzing, and K. Ploog*
Max-Planck-Institut für Festkörperforschung, Heisenbergstrasse 1, 70569 Stuttgart, Federal Republic of Germany
(Received 3 August 1993)

Coulomb blockade effects are investigated in lateral transport through a quantum dot defined in a two-dimensional electron gas. Tunneling through excited states of the quantum dot is observed for various tunneling barriers. It is shown that transport occurring via transitions between ground states with different numbers of electrons can be suppressed by the occupation of excited states. Measurements in a magnetic field parallel to the current give evidence for tunneling processes involving states with different spin.

PACS numbers: 71.50.+t, 71.70.Ej, 72.20.My, 73.40.Gk

The Coulomb interaction determines the behavior of electron transport through mesoscopic electronic systems weakly coupled with two electron reservoirs. Transport is inhibited if the energy necessary to add an additional electron to the mesoscopic island exceeds the electrochemical potential of the reservoirs and the thermal energy k_BT. This is known as the Coulomb blockade of tunneling [1]. For quantum dots realized in semiconductor nanostructures the discreteness of the energy spectrum also has to be taken into account. By increasing the voltage of a gate electrode, capacitively coupled to a quantum dot, the levels of the quantum dot are shifted in energy relative to the levels of the electron reservoirs, allowing the number of electrons enclosed in the quantum dot to increase one by one. Applying a magnetic field changes the energy necessary to add an electron to the quantum dot. Different techniques were used to measure this energy as a function of a magnetic field orientated perpendicularly to the plane of disklike quantum dots realized in AlGaAs/GaAs heterostructures [2,3]. Here we use magnetic fields orientated in the plane of the disk to resolve Zeeman spin splitting. This is combined with measurements at finite bias voltage between the reservoirs, where excited states of the confined electron system become accessible in transport, providing new tunneling channels [4–6]. Therefore, for the new magnetic field orientation we will present results of spectroscopy of the ground states *and* excited states of our system.

To define the quantum dot, metallic split gates, as shown schematically in the inset of Fig. 1, were deposited on the top of a Hall bar etched in a $GaAs/Al_{0.33}Ga_{0.67}As$ heterostructure with a 2DEG (electron density 3.4×10^{15} m^{-2}, mobility 60 m^2/V s at a temperature of 4.2 K). The diameter of the area between the tips of the gates is about 350 nm. In addition to these top gates, a metallic electrode (back gate) on the reverse side of the undoped substrate was used to change the electrostatic potential of the quantum dot. The distance between the 2DEG and the top gates was 86 nm, the distance between the 2DEG and the back gate was 0.5 mm. The sample was mounted in a ^{3}He/^{4}He dilution refrigerator with a base temperature of 22 mK. The two-terminal conductance through the quantum dot was measured by using an ac lock-in technique at a frequency of 13 Hz and an effective ac source-drain voltage of 5 μV. In addition to the ac source-drain voltage, a dc voltage V_{DS} in the range of mV could be applied. For the measurements, the top gates were kept at fixed voltages (around -0.7 V). The tunneling barriers could be tuned by slight changes in the voltage applied to the different top-gate fingers.

In Fig. 1, a typical curve of conductance versus back-gate voltage is shown. Only a few such well separated conductance resonances are observable in our system. For more negative back-gate voltages the conductance is completely suppressed, whereas for more positive back-gate voltages the widths of the conductance resonances are broadened and a finite conductance is measured between adjacent peaks.

In Fig. 2(a) the differential conductance dI/dV_{DS} is shown as a function of the back-gate voltage V_B for the different bias voltages V_{DS} (between -3 mV and 3 mV in 0.1 mV steps). In the linear grey-scale plot, white regions correspond to dI/dV_{DS} below -0.1 μS and black ones to dI/dV_{DS} above 2 μS. For clarity the main structures visible in Fig. 2(a) are sketched in Fig. 2(b). At vanishing V_{DS} the conductance resonances are observed. By increasing the absolute value of V_{DS}, the range in back-gate voltage V_B where transport through the quantum dot occurs is broadened linearly with $|V_{DS}|$. These regions of transport enclose almost rhombically shaped regions between them, where transport through the quantum dot

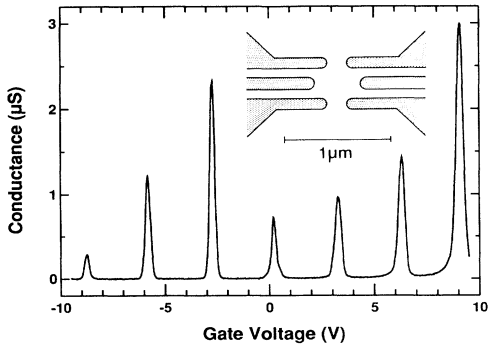

FIG. 1. Conductance versus back-gate voltage. Inset: Scheme of the center of split-gate structure used to define the quantum dot.

0031-9007/93/71(24)/4019(4)$06.00

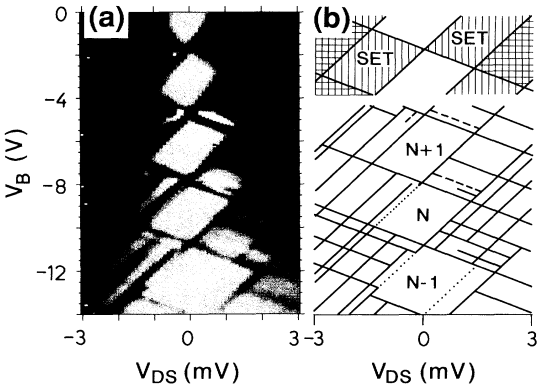

FIG. 2. (a) Differential conductance dI/dV_{DS} given in linear grey scale (white ≤ -0.1 μS, black ≥ 2 μS) as a function of back-gate voltage V_B for different bias voltages V_{DS}. (b) At the top: regions of SET are hatched, regions where the number of electrons can change by two at a time are cross-hatched. Lower part: The main structures visible in (a) are sketched. Dashed lines show regime of negative differential conductance; dotted lines show suppressed conductance.

is blocked [Coulomb blockade regime (CB)]. Here, the number of electrons in the quantum dot is fixed to an integer (e.g., to N), as the energy $\mu_{N+1}(V_B, V_{DS})$ necessary to add the next electron [the $(N+1)$th] to the quantum dot lies above the electrochemical potentials of the emitter (μ_E) and of the collector (μ_C), and the energy $\mu_N(V_{DS}, V_B)$ lies below μ_E and μ_C [7]. With N electrons enclosed in the quantum dot, the electrostatic potential of the quantum dot is continuously shifted up by sweeping the back-gate voltage V_B to positive values. Transport through the quantum dot from occupied states in the emitter to unoccupied states in the collector can begin when $\mu_{N+1}(V_B, V_{DS})$ falls below μ_E. As soon as $\mu_{N+1}(V_B, V_{DS})$ falls below μ_C by further increase in V_B, the number of electrons gets fixed to $N+1$. Thus the boundaries between transport and blockade regimes in the V_B vs V_{DS} plane are defined by the condition $\mu_E = \mu_{N+1}(V_B, V_{DS})$ and $\mu_{N+1}(V_B, V_{DS}) = \mu_C$, respectively, where $\mu_E - \mu_C = eV_{DS}$. As is visible in Fig. 2(a) these resonance positions shift linearly in V_B when changing V_{DS}, indicating that the confinement potential of the quantum dot is only weakly influenced by the small changes of V_B or V_{DS}. Thus, the shifts of the electrostatic potential of the quantum dot can be modeled by a capacitance circuit. From the two slopes dV_B/dV_{DS} characterizing the boundaries between transport and blockade, the scaling factor α between the change $\Delta\Phi$ of electrostatic potential and the change ΔV_B of back-gate voltage V_B is obtained [$\alpha = \Delta\Phi/\Delta V_B = (4.5 \pm 0.2) \times 10^{-4}$] [4]. This implies the difference $\mu_{N+1} - \mu_N$ in our dot to be around 1.3 meV. From the dot size the electron number in the dot is estimated to be about 50.

Because of the charging energy, the number of electrons in the quantum dot can change only one at a time in the transport regime neighboring the regime of blockade. This is called the regime of single-electron tunneling (SET) [hatched regions in the upper part of Fig. 2(b)]. At vanishing V_{DS} during transport, the quantum dot changes between the ground states of two electron systems (e.g., between a N and a $N+1$ electron system). At finite bias voltage, excited states for both electron systems also become accessible, providing new tunneling channels through the quantum dot. There are two possibilities: a new channel opens at the emitter side, or a new channel opens at the collector side. In the first case, an excited state of the $N+1$ electron system becomes accessible for putting the $(N+1)$th electron from the emitter to the N electron system in the quantum dot. In the second case, the quantum dot is left in an excited state of the N electron system, as the $N+1$th electron leaves the quantum dot to an unoccupied state in the collector. Both kinds of new channels are visible in Fig. 2 as additional structure within one SET regime and can be distinguished as the resonance position for the opening of a new channel from the emitter (to the collector) shifts to negative (positive) V_B with increasing $|V_{DS}|$ [4].

The distance of V_B positions between differential conductance peaks within one SET regime, shifting parallel in V_B when increasing $|V_{DS}|$, reveals the energy difference of states with the same number of electrons. This simple interpretation is true only if a fast and complete relaxation to the ground state of the confined electron system in the quantum dot occurs before the next tunneling process through one of the barriers starts. In this case the two systems (N or $N+1$ electrons) can be distinguished, allowing the spectroscopy of the $N+1$ electron system and of the N electron system separately within one SET regime. But, it has been shown that relaxation in zero-dimensional systems can be strongly suppressed [8]. Therefore, transitions between excited states of the N electron system and excited states of the $N+1$ electron system occur, making the interpretation more complex. The time in which relaxation can occur is roughly estimated by the mean time Δt between successive electrons passing through the quantum dot. From the mean height ΔI of current steps within the SET regime around $V_B = -12$ V in Fig. 2, we obtain $\Delta t = e/\Delta I = 0.5$ ns.

For the measurements shown in Fig. 2(a), the tunneling barriers were tuned to obtain (at vanishing bias voltage V_{DS}) a maximum amplitude for the conductance peak observable around $V_B = -5$ V in Fig. 2(a), i.e., to have resonant tunneling through symmetric barriers. In Fig. 3, measurements for asymmetric tunneling barriers are shown. Because of the capacitive coupling of the top gates to the quantum dot, the conductance peaks observed in the back-gate voltage are shifted. For asymmetric tunneling barriers the transport process through the quantum dot is expected to be governed by the tunneling process through the "thick" barrier (thick means "less coupling of the quantum dot to the neighboring lead"). For such a barrier the capacitance between the quantum

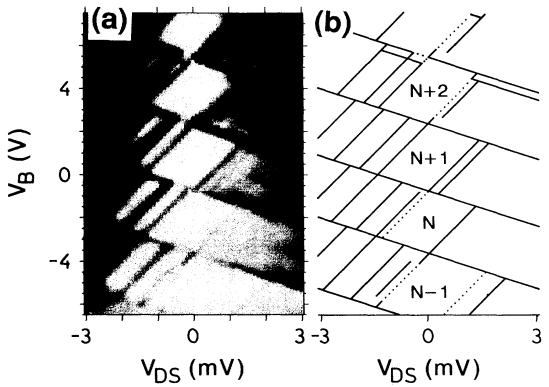

FIG. 3. (a) Same as for Fig. 2(a), but for asymmetric tunneling barriers. (b) The main structures visible in (a) are sketched. Dotted lines show suppressed conductance.

dot and the lead is decreased, as indicated in Fig. 3 by a change in the slopes characterizing the boundaries between transport and blockade regimes.

In Fig. 3, for negative bias voltages V_{DS}, electrons are injected into the quantum dot through the thick barrier, whereas for positive bias voltages, they are injected through the thin barrier. In contrast to the more symmetric case, where the opening of new channels at *both* barriers has the same importance (causing the gridlike structure within the SET regime in Fig. 2), here the conductance through the quantum dot is dominated by the thick barrier. Even more pronounced are the effects observed beyond the SET regime, where the number of electrons in the quantum dot could change, e.g., between $N-1$, N, and $N+1$ [$N+(1/N)/(N-1)$ regime, see for identification Fig. 2(b) where similar regions are crosshatched]. In Fig. 3 at negative V_{DS}, the structures indicating new transport channels in the $N+1/N$ regime (SET) stop at the boundary of the $N+(1/N)/(N-1)$ regime, since in this case the thick barrier is at the emitter side and the quantum dot is preferably filled with $N-1$ electrons. Thus, transitions from the $N-1$ to the N electron system dominate in the transport process. On the contrary, if the thick barrier is on the collector side, the quantum dot is filled up to $N+1$ electrons. Transitions from $N+1$ to N electrons dominate the transport.

The most striking features observable in Figs. 2 and 3 (dotted lines) indicate the interplay of transport channels opened on the emitter and the collector side leading to a suppression of conductance. For instance, the structure visible in Fig. 2(a) around $V_B = -12$ V at negative V_{DS} may be interpreted by the following: At small negative V_{DS}, the transport through the quantum dot occurs via transitions between the ground states of the $N-1$ and the N electron system. Going to negative V_{DS} and negative V_B by following the boundary between the transport and the blockade region ($N-1$ electrons enclosed in the dot), this transport channel becomes suppressed (dotted line) by a channel opened on the collector side (solid line which shifts to positive V_B with negative V_{DS}). Thus, the occupation of an excited state of the $N-1$ electron system blocks transport. Penetrating into the SET regime, an excited state of the N electron system becomes accessible (solid line which shifts to negative V_B with negative V_{DS}), again increasing the conductance.

Thus, the conductance through the quantum dot is not always increased but can also be decreased by accessing excited states. This is a property of the SET process: Using one channel blocks the transport through the other channels as the number of electrons in the quantum dot can be changed only one at a time. Electrons from the emitter reservoir compete in entering the quantum dot by different channels and then electrons in the quantum dot compete in leaving the quantum dot by different channels to the collector reservoir. The change of the conductance depends on the traversing time of the electrons through the dot via the different channels, and is also influenced by relaxation processes.

Within the SET regime, negative differential conductance (NDC) appears [white regions in Fig. 2(a), dashed lines in Fig. 2(b)] as also observed by Johnson *et al.* [5]. In our measurements the NDC peaks are shifting parallel to the boundaries of transport and blockade regimes, which again implies that the conductance through the quantum dot is decreased by accessing excited states as explained above. Pfaff *et al.* [9] modeled NDC by taking into account the different spin degeneracy and the spin selection rule for transition between states of the N and $N+1$ electron system.

To obtain more information about the different tunneling channels, measurements in a magnetic field B orientated parallel to the plane of the 2DEG and parallel to the current were performed. This orientation diminishes orbital effects, allowing us to follow a conductance peak up to high magnetic fields where Zeeman splitting of the energies of states with different spin quantum numbers is resolvable [at 15 T $g\mu_B B$ is 0.38 meV for the g factor of bulk GaAs ($|g| = 0.44$)]. In Fig. 4(a) the differential conductance measured at $V_{DS} = -0.7$ mV is plotted in grey scale (white $dI/dV_{DS} \leq -0.01$ μS, black $dI/dV_{DS} \geq 1$ μS) as a function of back-gate voltage V_B for the magnetic field values between -15 and 15 T in 0.5 T steps. The peak maxima visible in Fig. 4(a) are plotted in Fig. 4(b), indicating the resonance condition for opening a new channel. The tunneling barriers have been tuned at $B = 0$ T roughly to the situation of Fig. 2. The upper and lower boundaries of each SET regime show the same shift in V_B position with magnetic field as predicted by the conditions $\mu(V_{DS}, V_B^u, B) = \mu_C$ and $\mu(V_{DS}, V_B^l, B) = \mu_E$, where $\mu_E - \mu_C = eV_{DS}$ is magnetic field independent. At finite bias voltage the magnetic field dependence of a state which is a ground state in some range of the magnetic field can be followed into the range where this state has become an excited state. In Fig. 4(b) for the conductance resonance around $V_B = -4$ V, four arrows indicate magnetic field posi-

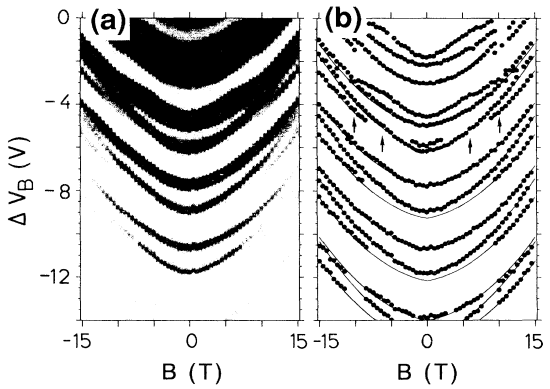

FIG. 4. (a) Differential conductance dI/dV_{DS} given in a linear grey scale (white ≤ -0.01 μS, black ≥ 1 μS) as a function of back-gate voltage V_B for different magnetic fields B. The bias voltage V_{DS} was -0.7 mV (see Fig. 2). (b) Positions of peak maxima visible in (a). The lines are fitted curves (as discussed in the text).

tions, where such transitions occur. In corresponding measurements at *vanishing* V_{DS}, where only transitions between the ground states are allowed, the shift of the V_B position of this conductance peak shows bends accompanied by an amplitude modulation at these magnetic field values. Several different magnetic field dispersions are observable but only two different dispersions can be followed over a magnetic field range large enough to enable a fit to be made to the data ($\alpha B^2 + \beta B$ with same α and different β). These two dispersions are found in all SET regimes [solid lines in Fig. 4(b)]. The difference in the shifts can be fitted linearly. This linear dependence suggests that the tunneling channels are due to states with different spin. Relating the difference in shift to the Zeeman splitting we obtain a g factor of $|g| = 0.31 \pm 0.04$. A splitting of the differential conductance peaks is not observed. Malcher *et al.* [10] calculated the spin splitting of levels in a 2DEG at $B = 0$ T due to the nonparabolicity of the bulk band structure of GaAs and spin-orbit coupling. This is in the range of a few tenths of a mV which is comparable to typical distances of energy levels observable here in our quantum dot. For the overall shift of the conductance resonances in V_B, the change in the chemical potential of the 2DEG has to be taken into account, which was discussed elsewhere [11].

The magnetic field dependence (Fig. 4) can now be compared with the results of Fig. 2, where suppression of the conductance is seen in several regions (dotted lines in Fig. 2). For instance, the feature observable around $V_B = -12$ V in Fig. 2 is interpreted by the following: The transition between the ground states of the $N-1$ and N electron system (channel 1) is suppressed because an excited state of the $N-1$ electron system has become accessible, blocking transport. The conductance is increased again when allowing the transition to an excited state of the N electron system (channel 2). The difference between the transition energies of the two channels increases linearly with magnetic field (Fig. 4). This suggests that states with different spin are responsible for the suppression of the conductance through the dot.

In summary, transport measurements through a single quantum dot in the single-electron-tunneling regime allow spectroscopy of ground and excited states. New tunneling channels opening at finite drain-source voltage are classified by their shift of position in the back-gate voltage when changing the bias voltage. Transport through new tunneling channels increases or decreases the total conductance through the quantum dot, depending on the interplay between the different channels. Different conductance channels show different dependence on a magnetic field parallel to the current, which we correlate to states with different spin.

We gratefully acknowledge stimulating discussions with D. Pfannkuche, R. Blick, H. Pothier, D. Weinmann, W. Häusler, J. J. Palacios, C. Tejedor, and P. Maksym. We thank M. Riek, A. Gollhardt, and F. Schartner for their expert help with the sample preparation. Part of the work has been supported by the Bundesministerium für Forschung und Technologie.

* Present address: Paul-Drude Institut für Festkörperelektronik, Hausvogteiplatz 5-7, 10117 Berlin, Germany.

[1] Special Issue on Single Charge Tunneling, in Z. Phys. B **85**, No. 3 (1991); *Single Charge Tunneling*, edited by H. Grabert and M.H. Devoret, NATO ASI Ser. B, Vol. 294 (Plenum, New York, 1992).

[2] P.L. McEuen, E.B. Foxman, U. Meirav, M.A. Kastner, Y. Meir, N.S. Wingreen, and S.J. Wind, Phys. Rev. Lett. **66**, 1926 (1991).

[3] R.C. Ashoori, H.L. Störmer, J.S. Weiner, L.N. Pfeiffer, S.J. Pearton, K.W. Baldwin, and K.W. West, Phys. Rev. Lett. **71**, 613 (1993).

[4] J. Weis, R.J. Haug, K. v. Klitzing, and K. Ploog, Phys. Rev. B **46**, 12837 (1992).

[5] A.T. Johnson, L.P. Kouwenhoven, W. de Jong, N.C. van der Vaart, C.J.P.M. Harmans, and C.T. Foxon, Phys. Rev. Lett. **69**, 1592 (1992).

[6] E.B. Foxman, P.L. McEuen, U. Meirav, N.S. Wingreen, Y. Meir, P.A. Belk, N.R. Belk, M.A. Kastner, and S.J. Wind, Phys. Rev. B **47**, 10020 (1993).

[7] L.P. Kouwenhoven, N.C. van der Vaart, A.T. Johnson, W. Kool, C.J.P.M. Harmans, J.G. Williamson, A.A.M. Staring, and C.T. Foxon, Z. Phys. B **85**, 367 (1991).

[8] U. Bockelmann and G. Bastard, Phys. Rev. B **42**, 8947 (1990); U. Bockelmann and T. Egeler, Phys. Rev. B **46**, 15574 (1992).

[9] W. Pfaff, D. Weinmann, W. Häusler, B. Kramer, and U. Weiss (to be published).

[10] F. Malcher, G. Lommer, and U. Rössler, Superlattices Microstruct. **2**, 267 (1986).

[11] J. Weis, R.J. Haug, K. v. Klitzing, and K. Ploog, Proceedings of the 10th International Conference on Electronic Properties of Two-Dimensional Systems, Newport, 1993 [Surf. Sci. (to be published)].

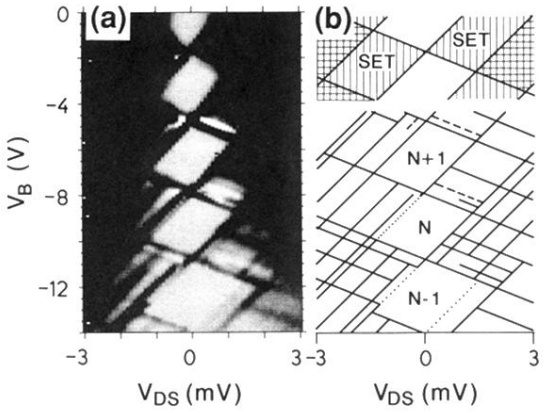

FIG. 2. (a) Differential conductance dI/dV_{DS} given in linear grey scale (white ≤ -0.1 μS, black ≥ 2 μS) as a function of back-gate voltage V_B for different bias voltages V_{DS}. (b) At the top: regions of SET are hatched, regions where the number of electrons can change by two at a time are cross-hatched. Lower part: The main structures visible in (a) are sketched. Dashed lines show regime of negative differential conductance; dotted lines show suppressed conductance.

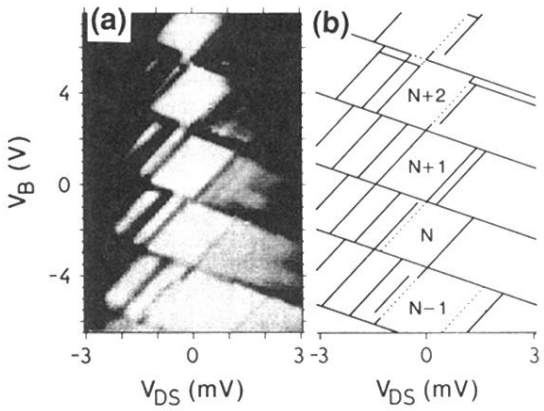

FIG. 3. (a) Same as for Fig. 2(a), but for asymmetric tunneling barriers. (b) The main structures visible in (a) are sketched. Dotted lines show suppressed conductance.

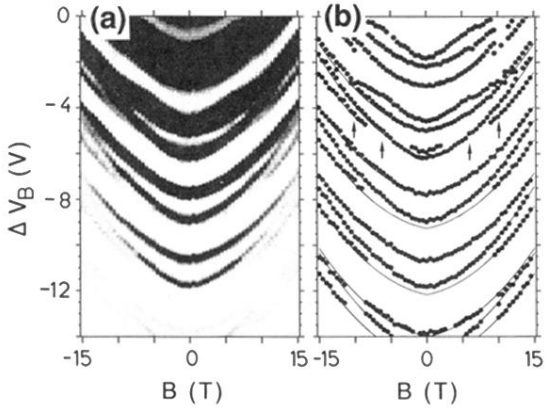

FIG. 4. (a) Differential conductance dI/dV_{DS} given in a linear grey scale (white ≤ -0.01 μS, black ≥ 1 μS) as a function of back-gate voltage V_B for different magnetic fields B. The bias voltage V_{DS} was -0.7 mV (see Fig. 2). (b) Positions of peak maxima visible in (a). The lines are fitted curves (as discussed in the text).